



Experimental Models of Short Courses of Liposomal Amphotericin B for Induction Therapy for Cryptococcal Meningitis

AQ: au **Jodi Lestner,^a Laura McEntee,^a Adam Johnson,^a Joanne Livermore,^a Sarah Whalley,^a Julie Schwartz,^b John R. Perfect,^c Thomas Harrison,^d William Hope^a**

AQ: aff Antimicrobial Pharmacodynamics and Therapeutics, Department of Molecular and Clinical Pharmacology, University of Liverpool, Liverpool, United Kingdom^a; Charles River Laboratories, Davis, California, USA^b; Department of Medicine, Duke University, Durham, North Carolina, USA^c; Research Centre for Infection and Immunity, St. George's University of London, London, United Kingdom^d

AQ: A

ABSTRACT Cryptococcal meningoencephalitis is a rapidly lethal infection in immunocompromised patients. Induction regimens are usually administered for 2 weeks. The shortest effective period of induction therapy with liposomal amphotericin B (LAMB) is unknown. The pharmacodynamics of LAMB were studied in murine and rabbit models of cryptococcal meningoencephalitis. The concentrations of LAMB in the plasma and brains of mice were measured using high-performance liquid chromatography (HPLC). Histopathological changes were determined. The penetration of LAMB into the brain was determined by immunohistochemistry using an antibody directed to amphotericin B. A dose-dependent decline in fungal burden was observed in the brains of mice, with near-maximal efficacy achieved with LAMB at 10 to 20 mg/kg/day. The terminal elimination half-life in the brain was 133 h. The pharmacodynamics of a single dose of 20 mg/kg was the same as that of 20 mg/kg/day administered for 2 weeks. Changes in quantitative counts were reflected by histopathological changes in the brain. Three doses of LAMB at 5 mg/kg/day in rabbits were required to achieve fungicidal activity in cerebrospinal fluid (cumulative area under the concentration-time curve, 2,500 mg · h/liter). Amphotericin B was visible in the intra- and perivascular spaces, the leptomeninges, and the choroid plexus. The prolonged mean residence time of amphotericin B in the brain suggests that abbreviated induction regimens of LAMB are possible for cryptococcal meningoencephalitis.

KEYWORDS liposomal amphotericin B, pharmacokinetics, pharmacodynamics, *Cryptococcus neoformans*, cryptococcal meningitis, meningoencephalitis

AQ: B

AQ: C

Cryptococcal meningitis is a common and frequently lethal disease in patients with HIV/AIDS (1). Rapid fungicidal activity in cerebrospinal fluid (CSF) is associated with better clinical outcomes and improved survival (2). Amphotericin B deoxycholate (DAMB) is the most potent amphotericin B formulation on a milligram-milligram basis (3, 4). While effective, DAMB is toxic and associated with significant infusion-related toxicity, nephrotoxicity, and anemia (5, 6). Furthermore, DAMB is not orally bioavailable and must be injected. The need for rapid, reliable monitoring for side effects and for intravenous administration means that amphotericin B-based treatment is simply not possible in many resource-poor settings. Hence, the best current therapy cannot be administered to patients in many countries where the prevalence of cryptococcal meningitis is the highest. In these cases, the only alternative agent is fluconazole, but even with the use of high doses (800 to 1,200 mg/day), the fungicidal activity in CSF

Received 16 January 2017 Returned for modification 13 February 2017 Accepted 4 March 2017

Accepted manuscript posted online ●●●

Citation Lestner J, McEntee L, Johnson A, Livermore J, Whalley S, Schwartz J, Perfect JR, Harrison T, Hope W. 2017. Experimental models of short courses of liposomal amphotericin B for induction therapy for cryptococcal meningitis. *Antimicrob Agents Chemother* 61:e00090-17. <https://doi.org/10.1128/AAC.00090-17>.

Copyright © 2017 American Society for Microbiology. All Rights Reserved.

Address correspondence to Jodi Lestner, jlestner@liverpool.ac.uk.

and clinical outcomes are suboptimal (7, 8). Alternative approaches are urgently required.

There is surprisingly little evidence for the use of liposomal amphotericin B (LAMB) for cryptococcal meningitis. Preclinical and clinical data suggest that 3 to 6 mg/kg of body weight/day is a safe and effective regimen (9, 10). Typically, the duration of amphotericin B-based induction regimens is 2 weeks, based primarily on surrogate mycological markers of early fungicidal activity such as CSF sterilization (11, 12). The shortest duration of LAMB that is maximally effective is not known. We recently demonstrated that an abbreviated course of DAMB (3 days) may be as effective as 2 weeks of therapy (13) and that short courses of DAMB (in combination with fluconazole) are associated with rapid clearance of the CSF in patients with cryptococcal meningitis (14). Thus, there are a precedent and a rationale for examining the safety and efficacy of abbreviated regimens of LAMB as induction therapy for cryptococcal meningitis.

Here, we used two previously described (15, 16) and well-characterized laboratory animal models of cryptococcal meningitis to study the pharmacodynamics of abbreviated courses of liposomal amphotericin B. Our principal goal was to provide the experimental evidence underpinning phase II and III clinical trials examining the efficacy of abbreviated regimens of LAMB.

RESULTS

Dose exposure-response relationships in mice. Liposomal amphotericin B was well tolerated in mice with no observed toxicity following rapid intravenous (i.v.) injection. There was a clear dose-response relationship with doses of 0.5 to 20 mg/kg/day. Fungicidal activity was not observed (i.e., we did not observe a decline in the number of log₁₀ CFU/g following daily therapy). Rather, a fungistatic effect was seen whereby the infection at the time of drug administration 24 h postinoculation was stabilized. Near-maximal antifungal activity was observed following treatment with 10 to 20 mg/kg/day and with an AUC/MIC ratio of approximately 100 (Fig. 1).

A profound and durable antifungal effect was apparent following a single dose of 20 mg/kg in mice (Fig. 2). There was no evidence of significant fungal regrowth after 240 h of observation. The persistent antifungal effect may be explained by the long terminal half-life of amphotericin B in the plasma and cerebrum (~113 h) (Fig. 3).

Histopathology and immunohistochemistry in mice. The persistent antifungal effect evident from the log₁₀ CFU/g data were mirrored by the histopathological findings shown in Fig. 4. In mice receiving vehicle only, cryptococcal meningoencephalitis manifested as a multifocal disease with cyst-like cavities filled with multiple encapsulated organisms approximately 6 to 10 μm in diameter. There was no evidence of an inflammatory component within or around the cavities.

Mouse livers (harvested from mice receiving a total cumulative liposomal amphotericin B dose of 225 mg/kg) were used as the positive-control tissue in all amphotericin B localization experiments. Moderate to marked staining of frequent Kupffer cells was observed in the positive-control tissue. All other tissue elements were negative. There was no staining of Kupffer cells when a species-, isotype-, and concentration-matched negative-control antibody (rabbit IgG) was substituted for the rabbit anti-AMB reagent. Kupffer cells in control mouse liver tissue that received 5% dextrose did not stain with rabbit anti-AMB reagent.

There was differential penetration of amphotericin B into the brain (Fig. 5). Staining was apparent early (i.e., 1 h after dose) and in both intravascular and perivascular spaces, suggesting that the drug crossed the blood-brain barrier. Staining was especially prominent in blood vessels in the leptomeninges and choroid plexus, as well as small cerebral capillaries. Staining was both extra- and intracellular. Granular extracellular staining was observed in and surrounding blood vessels. Intracellular cytoplasmic staining was observed in mononuclear/microglial cells. Positive circulating mononuclear cells (presumptive monocytes) were identified in cerebral capillaries. Additional extracellular staining was observed in the ventricular system associated with the

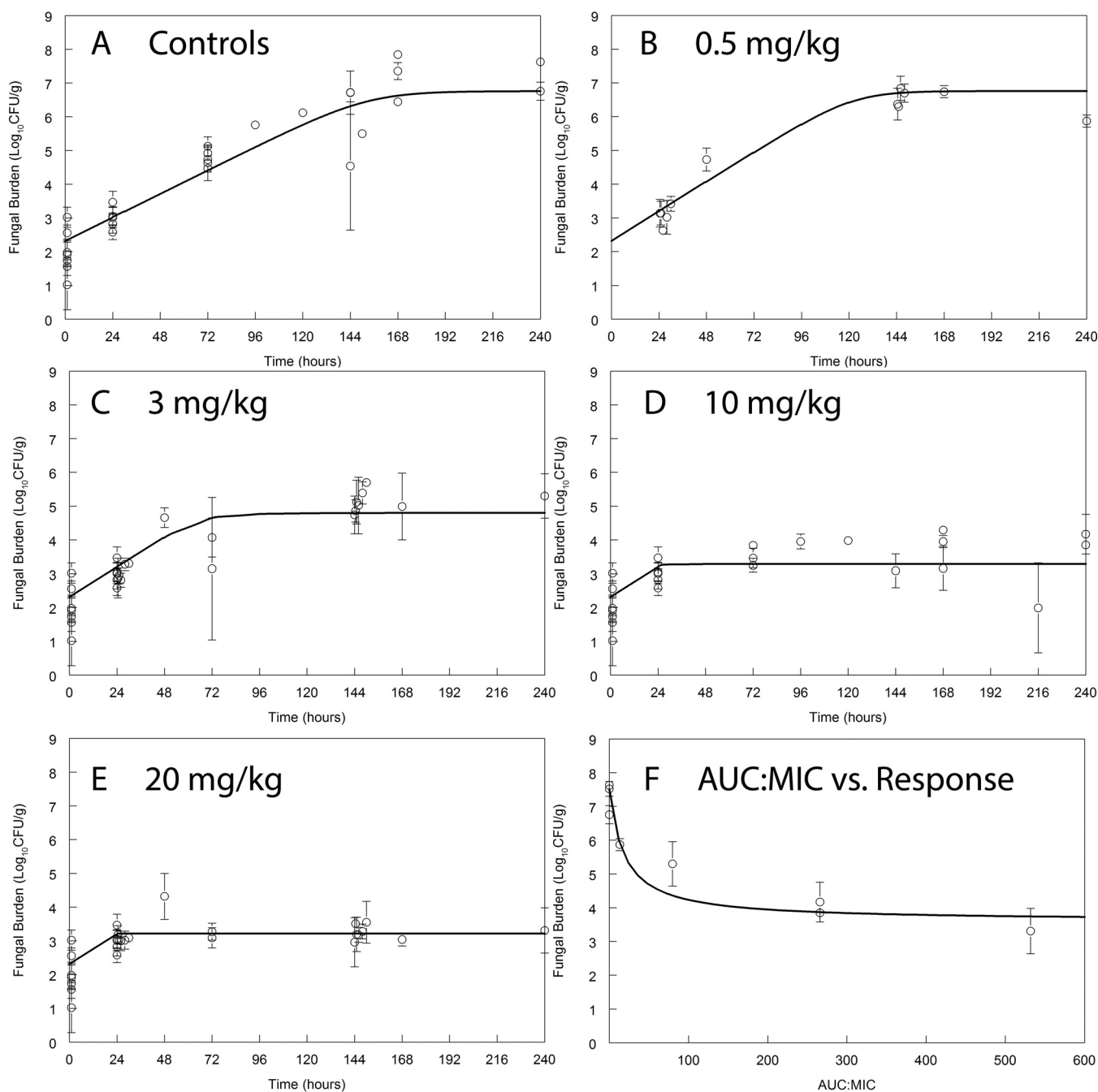


FIG 1 Pharmacodynamics of LAMB in cohorts of mice receiving 0.5 (B), 3 (C), 10 (D), and 20 (E) mg/kg/day i.v. The AUC/MIC ratio at steady state versus the observed fungal density at the end of the experiment (time = 240 h) is shown in panel F. All data are means \pm standard deviations of results from groups of three mice.

ependymal lining, suggesting entry into the CSF. In contrast, staining was not observed in the normal cerebral tissue or in residual cryptococcomas after 10 days of treatment with LAMB at doses of 10 or 20 mg/kg/day.

Mathematical PK-PD model in mice. The fit of the mathematical model to the combined murine pharmacokinetic-pharmacodynamic (PK-PD) data set was acceptable, even though fitting was difficult. The estimates for the parameters are summarized in Table 1. The principal challenge was modeling the depot-like effect of LAMB in the brains of mice in which low drug concentrations were observed to have exerted an antifungal effect that lasted well beyond the time that liposomal amphotericin B concentrations were detectable.

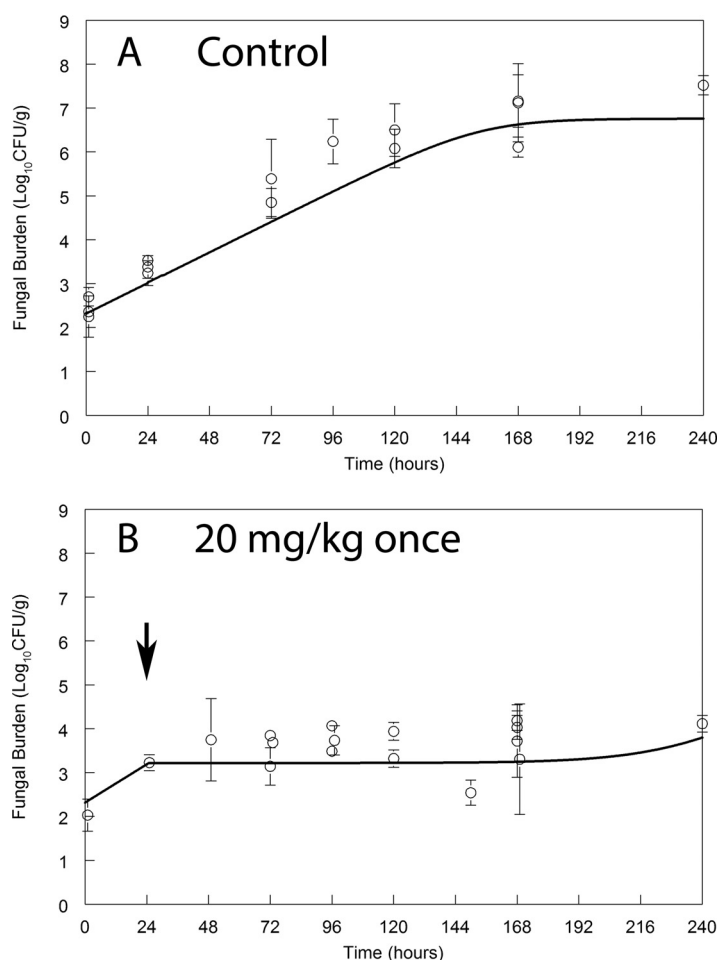


FIG 2 Pharmacodynamics of vehicle control (A) and LAMB (B) following the administration of a single dose of 20 mg/kg i.v. to mice with cryptococcal meningoencephalitis. Data are the means \pm standard deviations of results from groups of three mice. The solid line represents the fit of the mathematical PK-PD model (parameters summarized in Table 1). The black arrow denotes the time of drug administration relative to inoculation (which occurred at time zero).

PK-PD relationships in rabbits. The mean parameter values best accounted for the observed PK data. The parameter values were as follows: clearance of drug from the central compartment (CL_c), 0.018 ± 0.008 liters/h; first-order rate constant connecting the central and peripheral compartments (K_{cp}), 10.37 ± 0.416 h⁻¹; first-order rate constant connecting the peripheral and central compartments (K_{pc}), 26.09 ± 0.96 h⁻¹; first-order rate constant (K), 0.093 ± 0.04 h⁻¹; initial volume (V_{in}), 4.717 ± 0.233 liters; and final volume (V_{fn}), 0.003 ± 0.002 liters. The coefficients of determination for the linear regression before and after the Bayesian step were 0.87 and 0.98, respectively, and in both cases, the intercept and slope approximated zero and one, respectively.

The pharmacodynamics data in rabbits similarly illustrated the potential utility of abbreviated LAMB induction but differed somewhat from those observed in mice. A single dose of LAMB at 5 mg/kg appeared fungistatic only up to 264 h and did not provide a durable response in the CSF or cerebrum ($\Delta\log_{10}$ CFU/g = 1.9 ± 1.2 and 3.2 ± 0.5 , respectively), despite a higher estimated AUC from 0 to 24 h (AUC_{0-24}) than that in mice receiving a single dose of 20 mg/kg (820 ± 15 versus 580 ± 30 mg \cdot h/liter). Three doses of LAMB at 5 mg/kg administered every 24 h (and commencing 48 h postinoculation) induced a prompt decline in fungal burden in the CSF and cerebrum ($\Delta\log_{10}$ CFU/ml = -2.8 ± 0.8 and -0.1 ± 0.4 , respectively). This regimen produced a cumulative total AUC_{48-120} of 2,499 mg \cdot h/liter. The effect of this abbreviated regimen in rabbits was comparable to that achieved with daily therapy (Fig. 6).

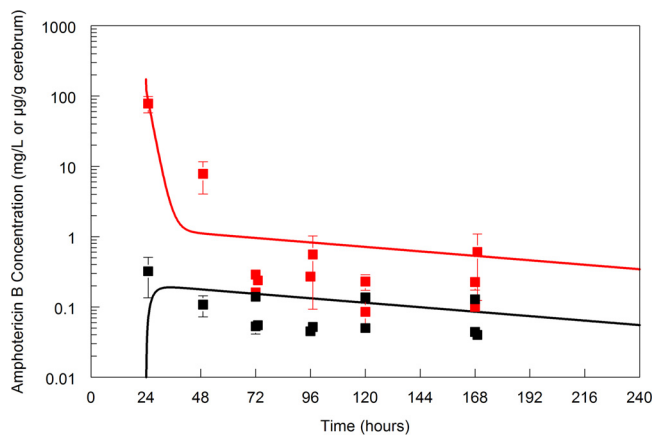


FIG 3 Pharmacokinetics of LAMB in murine plasma (red line and red data points) and cerebrum (black line and black data points) in cohorts of mice infected with *Cryptococcus neoformans* receiving LAMB at 20 mg/kg once i.v. (24 h postinoculation). All data are means \pm standard deviations of results from groups of three mice. The terminal half-life in the plasma and cerebrum is approximately 133 h.

The exposure-response relationships in the cerebra of rabbits were similar. The fungal densities for control rabbits and for rabbits receiving 5 mg/kg once, 5 mg/kg/day for 3 days, and 5 mg/kg/day were 5.92 ± 0.55 , 5.21 ± 1.20 , 2.43 ± 1.23 , and 2.47 ± 0.70 log₁₀ CFU/g (mean \pm standard deviation), respectively. Thus, in comparison to the murine studies, >1 day of therapy was required in rabbits to achieve fungicidal activity in the cerebrum and CSF.

PK-PD targets and bridging studies. A human regimen of liposomal amphotericin B of 4 mg/kg/day produces an AUC_{0–24} at steady state of ~190 mg \cdot h/liter. As can be seen in Fig. 1F, this is associated with near-maximal antifungal efficacy in mice receiving daily liposomal amphotericin B. A single dose of 20 mg/kg in mice (AUC_{0–24}, 550 to 600 mg \cdot h/liter) also produced near-maximal antifungal activity. The bridging study in

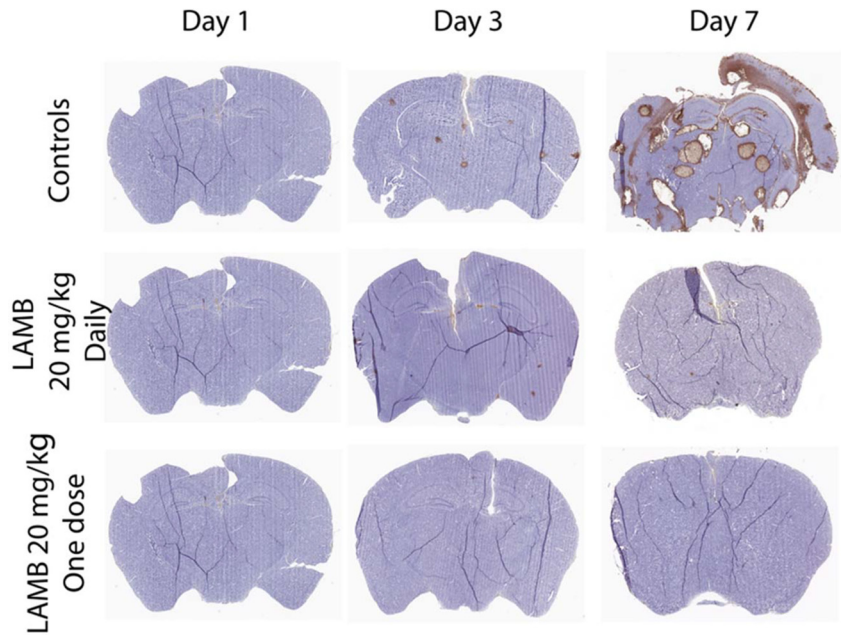


FIG 4 Representative cross-sections of brains from mice receiving vehicle control, LAMB at 20 mg/kg/day i.v., and LAMB at 20 mg/kg once i.v. Each section was stained with an anticryptococcal antibody and then counterstained with hematoxylin. Treatment was initiated at the end of day 1 (i.e., 24 h postinoculation). There are multiple cryptococcomas at the end of day 7 in untreated controls. In contrast, there are relatively few and exceedingly small lesions in the two treatment groups.

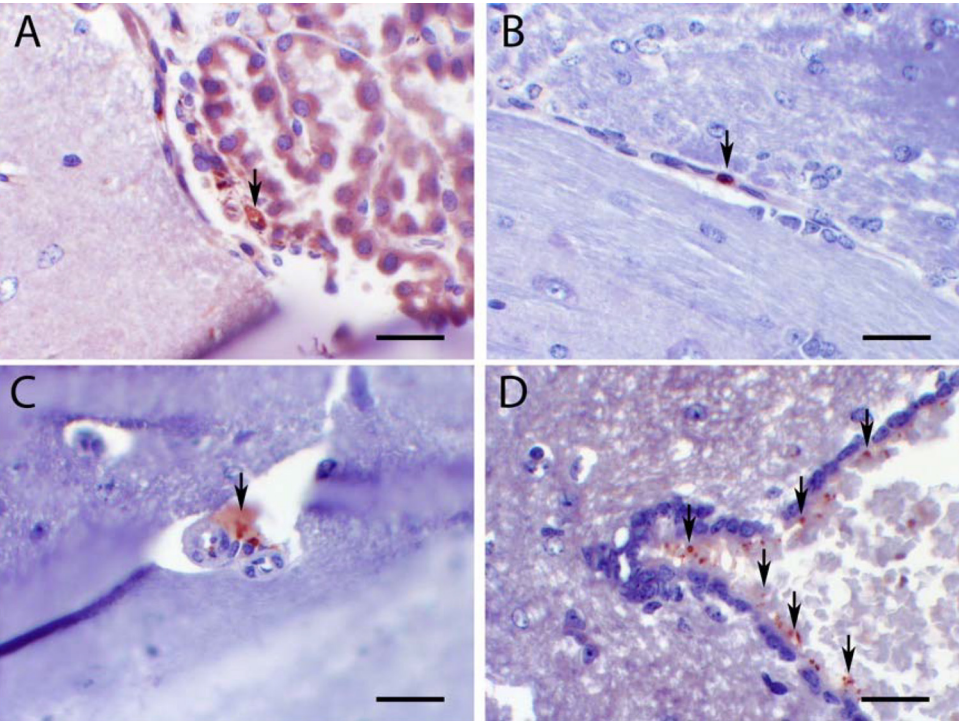


FIG 5 Distribution of LAMB in the central nervous system. All mice received LAMB at 20 mg/kg i.v. In each panel, black arrows indicate areas of staining of amphotericin B. (A) LAMB staining in the choroid plexus (extracellular and within a macrophage); (B) positive LAMB staining within a mononuclear cell in a thin-walled cerebral capillary; (C) positive staining in a perivascular location, adjacent to a thick-walled small arteriole; (D) LAMB staining in CSF associated with the apical surface of ependymal cells, cerebral aqueduct. Scale bars, 5 (A, B, and D) and 25 (C) μ m.

rabbits suggested that a single dose of 5 mg/kg (AUC, 833 mg · h/liter) was insufficient to achieve fungicidal activity. Rather, a total of three doses of 5 mg/kg/day (cumulative AUC, 2,499 mg · h/liter) was required to achieve fungicidal activity in the CSF. Thus, there was a degree of discordance between the pharmacodynamic targets from mice and rabbits, with the latter requiring slightly more drug exposure to achieve the same effect.

DISCUSSION

Amphotericin B is the most potent agent for induction therapy against *Cryptococcus neoformans*, and the combination with flucytosine results in the most rapid overall decline in fungal burden (17). This study suggests that abbreviated regimens of

TABLE 1 Parameters from the population PK-PD model from mice^a

| Parameter (unit) | Value | | |
|--|------------|------------|---------|
| | Mean | Median | SD |
| CL _S (liters/h) | 0.00082 | 0.00094 | 0.00018 |
| Vol (liters) | 0.003 | 0.0027 | 0.0019 |
| K _{cp} (h ^{−1}) | 11.99 | 10.52 | 9.94 |
| K _{pc} (h ^{−1}) | 15.70 | 23.33 | 11.41 |
| K _{cb} (h ^{−1}) | 0.16 | 0.22 | 0.013 |
| K _{bc} (h ^{−1}) | 0.034 | 0.01 | 0.038 |
| K _{g max} (log ₁₀ CFU/g/h) | 0.096 | 0.084 | 0.033 |
| H _g | 7.96 | 7.72 | 6.00 |
| C _{50 g} (mg/liter) | 0.088 | 0.056 | 0.100 |
| Pop _{max} (CFU/g) | 23,785,100 | 57,435,030 | 249,007 |
| V _m (liters) | 0.72 | 0.94 | 0.37 |
| Initial condition (CFU/g) | 186 | 207 | 133.97 |

^aEstimates for the mean, median, and standard deviation (SD) are shown. See the text for descriptions of parameters.

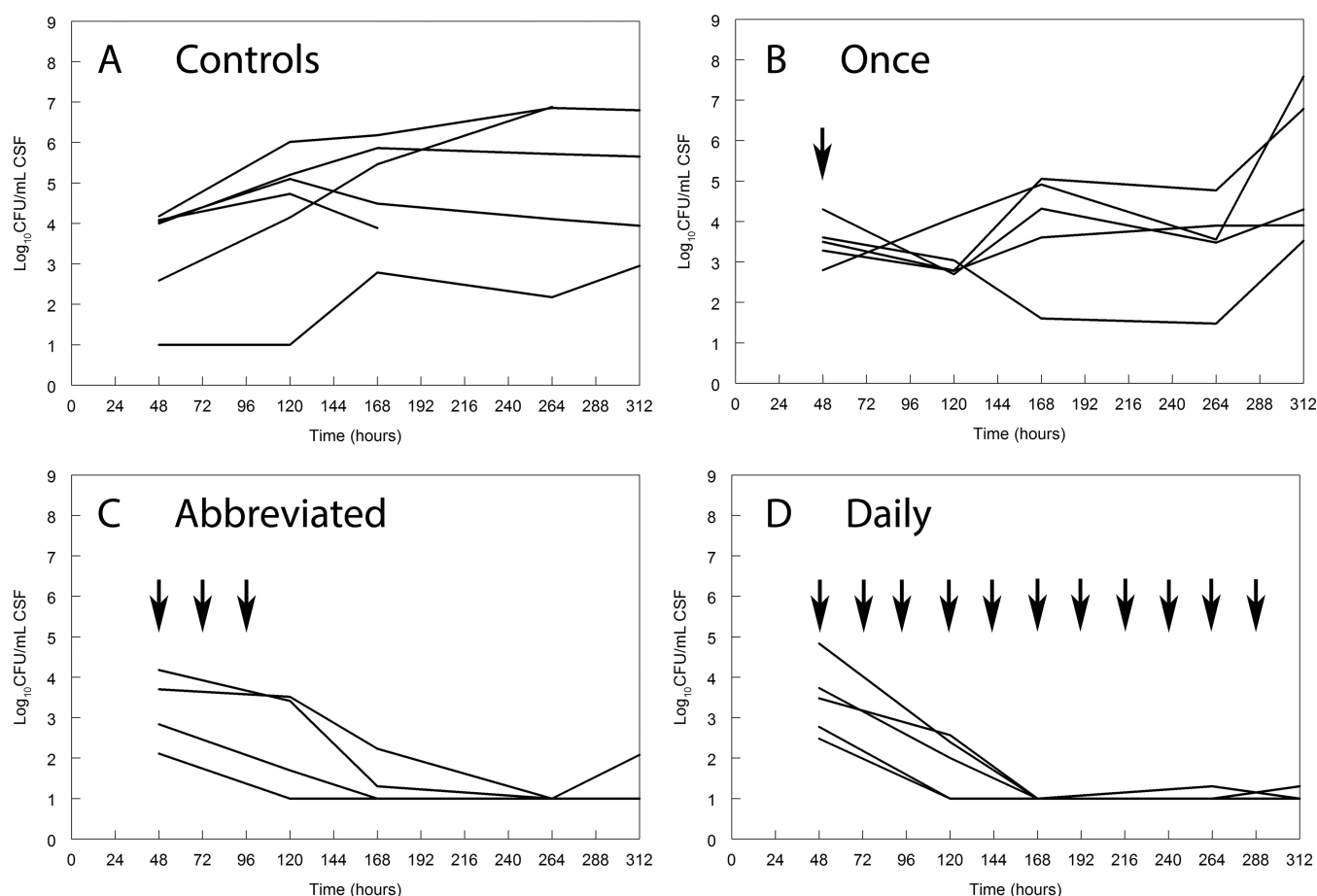


FIG 6 Time course of fungal density in the CSF of rabbits following various regimens of liposomal amphotericin B. Each line represents the data from a single rabbit. Each animal received 5 mg/kg every 24 h. The time course of fungal density in the CSF in rabbits receiving a single dose of drug (B) is comparable to that of controls (A). An abbreviated regimen of 5 mg/kg/day for three doses results in prompt fungicidal activity that is comparable to that achieved with daily therapy with the same dose.

liposomal amphotericin B may be feasible. This is primarily a function of a favorable pharmacokinetic profile with long terminal elimination phases in both the plasma and brain (half-life [$t_{1/2}$], 133 h).

The apparent discordance between plasma concentrations of liposomal amphotericin B and its persistent anticytotoxic activity in the central nervous system (CNS) of both mice and rabbits is of considerable interest, although the underlying mechanism driving this phenomenon is not entirely clear. One possibility is that there are a limited number of binding sites for amphotericin B in the CNS. Once occupied, amphotericin B does not readily disengage from its binding sites, leading to a pharmacologically active depot of drug. A relatively short course of liposomal amphotericin B (e.g., 1 to 3 doses) is all that is required to fully occupy these binding sites and result in persistent antifungal activity. Further doses are simply redundant and only serve to increase the probability of toxicity. The persistent occupation of receptors results in a sustained antifungal response for many days, even after plasma concentrations have declined to undetectable levels.

Exactly how liposomal amphotericin B traffics into the various clinically relevant effect sites is not clear. The drug penetrates into CNS subcompartments that are structurally normal and with histological evidence of inflammation (e.g., the ependyma shown in Fig. 5D). The immunohistochemistry studies suggest that the transfer from blood to the CNS occurs relatively quickly (i.e., in the first 24 h), but they do not enable estimates of the rate of transfer of drug. We did not observe high concentrations of drug within cryptococcomas, where the blood-brain barrier is likely significantly dis-

rupted, even though amphotericin B was readily quantifiable in homogenates of cerebral tissue of mice. This is probably because the amphotericin B immunoassay is relatively insensitive. We did not see any evidence of the drug being carried into cryptococcomas by inflammatory cells (the dump truck phenomenon), as is described for macrolides (18), although there was a very limited inflammatory response in this model.

While the study provides the experimental foundation for the concept of using abbreviated induction regimens of liposomal amphotericin B for cryptococcal meningitis, there is some uncertainty about the best regimen(s) for humans. Taken in isolation, the rabbit studies suggest that more than a single dose is required (with a cumulative AUC of $>833 \text{ mg} \cdot \text{h/liter}$). The AUC associated with an i.v. dose of 5 mg/kg in a rabbit is higher than that observed following administration of 20 mg/kg i.v. to a mouse (833 versus 555 $\text{mg} \cdot \text{h/liter}$, respectively), for which prolonged antifungal activity in the cerebrum was observed (Fig. 1). Thus, the mouse studies may underestimate the total (cumulative) drug exposure required for fungicidal activity in humans. Estimates of appropriate regimens are further complicated by some uncertainty in the PK of higher doses of liposomal amphotericin B in humans. We recently described much greater drug exposures (maximum concentration of drug in serum [C_{max}] and AUC) after multiple doses in at least some children receiving up to 10 mg/kg of LAMB (19), although we did not observe this phenomenon with intermittent high doses in adults (20). Further detailed PK studies of higher doses of LAMB are warranted.

The current study has several limitations and assumptions. First, we did not examine whether immunological effectors may have had an antifungal effect in addition to that of LAMB and whether this may have contributed to persistent antifungal activity observed with single doses. There was no evidence from the histopathological studies of an inflammatory infiltrate in either mice or rabbits (the latter is not shown). We extensively investigated this possibility in a recent study that examined the effect of abbreviated regimens of DAMB for cryptococcal meningoencephalitis, in which there was no evidence of immune-mediated antifungal killing (13). Second, we made an explicit assumption that the trafficking (both the rate and extent) of drug from the bloodstream to the site of infection is the same in mice, rabbits, and humans. Such an assumption is central to PK-PD bridging studies for all drug-pathogen combinations. In the majority of cases, this assumption is reasonable, but there are isolated examples where it is not (21). Third, there remains a degree of uncertainty regarding the lowest dose and shortest possible course of LAMB that is likely to be effective for patients with cryptococcal meningoencephalitis. We did not design this study to specifically address this question, which would have required many more animals. Finally, we did not examine optimal combinations of antifungal agents when one or both agents is administered as a short course.

Given the overwhelming cost and feasibility advantages of abbreviated induction therapy based on one or few doses of LAMB, clinical trials are now required to further test these ideas. A two-stage adaptive open-label phase II/III randomized noninferiority trial comparing alternative short-course LAMB regimens is under way and will be reported in 2017 (trial registration number ISRCTN10248064). These clinical trials will provide information for new therapeutic options for this neglected infection.

MATERIALS AND METHODS

Strain and *in vitro* susceptibility testing. *Cryptococcus neoformans* var. *grubii* (ATCC 208821 or H99) was the challenge organism for experiments in mice and rabbits. The MIC testing was performed using European Committee on Antimicrobial Susceptibility Testing (EUCAST) and Clinical and Laboratory Standards Institute (CLSI) methodology. MICs were determined in three independently conducted experiments.

Laboratory animal models of cryptococcal meningoencephalitis. All murine studies were performed under UK Home Office project license PPL 40/3630 and had received prior approval by the ethics committee at the University of Liverpool. Two models of cryptococcal meningitis that provide complementary information on the time course of cryptococcal meningoencephalitis, and the response to treatment with LAMB, were used. The murine model has the advantage of being highly reproducible. In

this model, the fungal burden in the cerebrum is the primary readout and quantitative counts in the CSF cannot be obtained. In contrast, the rabbit model enables the time course of fungal burden in the CSF, which is a clinically relevant subcompartment within the central nervous system, to be determined. The fungal burden in other central nervous system subcompartments is also available (e.g., cerebrum, vitreous, meninges) but only at the time of sacrifice.

For the murine model, immunosuppression is not required because mice are inherently susceptible to disseminated cryptococcal infection. An inoculum of 3×10^8 CFU in 0.25 ml phosphate-buffered saline (PBS) was injected i.v. via the lateral tail vein, which results in a highly reproducible encephalitis. Mortality occurs in the latter part of the second week of infection, meaning that early death does not confound any assessment of fungal burden in the initial 7 to 10 days of infection. The intended inoculum was confirmed by using quantitative counts after each experiment. The limit of detection for quantitative culture was $1.2 \log_{10}$ CFU/g.

A rabbit model of cryptococcal meningoencephalitis that was originally developed and described by Perfect et al. (15) was used to study the impact of abbreviated regimens on the time course of fungal burden in the CSF. Briefly, *C. neoformans* inocula were grown in yeast extract-peptone-dextrose (YPD) broth to a final concentration of $(3 \pm 0.25) \times 10^8$ CFU/ml. Inoculum concentrations were estimated by optical density and confirmed by quantitative culture. Anesthetized rabbits were infected via cisternal injection with an inoculum volume of 0.3 ml. Rabbits were anesthetized at day 2, 5, 7, and 11 postinoculation. CSF was obtained via cisternal puncture. A 1-ml sample was removed at each time point. All rabbits were sacrificed at the end of the experiment, which was 13 days postinoculation. A final CSF sample was obtained immediately after sacrifice. In addition, the fungal burden in the cerebrum at the end of the study period was determined as an additional endpoint. Representative samples of cerebrum were homogenized in 2 ml of PBS. Homogenate and CSF were then plated onto Sabouraud dextrose agar (SDA) containing chloramphenicol.

PK-PD studies. The PK-PD relationships in mice were determined over the course of multiple, independently conducted experiments. The time course of infection in the cerebrum was determined using a destructive design in which groups of CD-1 mice ($n = 3$ per group) were sacrificed at predefined intervals between 0 and 240 h postinoculation. Treatment was commenced 24 h postinoculation. Dose finding studies were conducted using 0.5 to 20 mg/kg/day. Each experiment incorporated an untreated control and at least two experimental arms ($n = 15$ per arm). Each dosing regimen was repeated in triplicate. Data from subjects requiring sacrifice on humane grounds were included in analyses at the time of death.

The PK data in plasma and cerebrum were determined in a separate experiment and once the relevant dose-response relationships had been determined. The PK was determined in infected mice. PK data were obtained at two intervals (immediately following the initiation of therapy and then after 5 days of dosing). Groups of mice ($n = 3$) were sacrificed 0.5, 1, 2, 6, and 24 h after drug administration. Plasma was obtained by terminal cardiac puncture, placed immediately on ice, centrifuged, and stored at -80°C for analysis. The cerebrum was extracted at the time of necropsy under sterile conditions. One hemisphere was submitted for quantitative cultures, while the other was stored for future measurement of amphotericin B concentrations.

PK-PD relationships were studied following various induction regimens, as follows. A single dose of 5 mg/kg was studied based on previous studies in invasive pulmonary aspergillosis. Groups of rabbits received a single dose, 3 doses of 5 mg/kg/day, and daily therapy of 5 mg/kg/day.

Measurement of amphotericin B concentrations. The concentrations of amphotericin B were estimated using a previously described assay (3). The limit of detection was 0.05 mg/liter. The intra- and interday variation was $<7\%$.

Histopathology and staining of LAMB in the CNS of mice. The brain was collected and placed into 10% neutral buffered formalin for histopathologic evaluation. Formalin-fixed tissues were trimmed, cryoprotected by sucrose replacement, and then embedded in OCT freezing medium. Approximately 5- μm sections were prepared for staining.

A commercially available mouse monoclonal antibody directed against *Cryptococcus neoformans* was used to determine the extent of infection (MyBioSource, LLC, San Diego, CA). Yeasts stained consistently and intensely (4+) positive with the anti-*C. neoformans* antibody. The yeasts did not stain with the species-, isotype-, and concentration-matched negative-control antibody (mouse IgG1) that was substituted for the mouse anti-*C. neoformans* reagent (data not shown).

Amphotericin B was visualized using an affinity-purified rabbit anti-amphotericin B antibody (Antibodies Inc., Davis, CA). Immunohistochemistry was performed using standard immunoperoxidase and alkaline phosphatase methodology and validated by appropriate and reproducible positive and negative controls for staining amphotericin B as previously described (22, 23).

Mathematical modeling. The murine PK and PD data from mice were modeled using a population methodology with the program Pmetrics (24). The mean drug concentration, cerebral concentration, and fungal burden in the cerebrum from groups of three mice were used. All data were weighted by the observed variance from each group of mice for drug concentrations and fungal burden. The structural model took the form:

$$\frac{dX_1}{dt} = R_1 - \left(\frac{CL_S}{V_C} + K_{cp} + K_{cb} \right) \times X_1 + K_{bc} \times X_3 + K_{pc} \times X_2 \quad (1)$$

$$\frac{dX_2}{dt} = -K_{pc} \times X_2 + K_{cp} \times X_1 \quad (2)$$

$$\frac{dX_3}{dt} = K_{cb} \times X_1 - K_{bc} \times X_3 \quad (3)$$

$$\frac{dN}{dt} = K_{g \max} \times \left(1 - \left(\frac{\frac{X_3 H_g}{V_m}}{\frac{X_3 H_g}{V_m} + C_{50g} H_g} \right) \right) \times \left(1 - \frac{N}{\text{Pop}_{\max}} \right) \times N \quad (4)$$

where X_1 , X_2 , and X_3 represent the amounts of amphotericin B (in milligrams) in the central compartment, peripheral compartment, and cerebrum, respectively. N is the number of organisms in the cerebrum. R_1 represents the i.v. injection of liposomal amphotericin B in milligrams; K_{cb} , K_{bc} , K_{cp} , and K_{pc} represent the first-order rate constants connecting the central (c), peripheral (p), and cerebrum (brain [b]) compartments. H_g is the slope function for the suppression of growth. $K_{g \max}$ is the maximum rate of fungal growth in the brain, V_m is the volume of the murine brain, V_c is the volume of the central compartment, C_{50g} is the concentration of amphotericin B in the brain at which there is half-maximal inhibition of growth, and Pop_{\max} is the maximum theoretical density of organisms in the brain.

Equation 1 describes the movement of liposomal amphotericin B into and out of the central compartment (plasma). Equation 2 describes the movement of liposomal amphotericin B into and out of the peripheral compartment. Equation 3 describes the movement of drug into the brain. Equation 4 describes the pharmacodynamics of amphotericin B. This equation contains terms that describe the capacity-limited fungal growth in the brain and drug-induced suppression of the fungal growth.

The fit of the mathematical model to the combined PK and PD data set from mice was assessed using the log likelihood value, measures of precision and bias, visual inspection of the observed-versus-predicted values both before and after the Bayesian step, and assessment of the linear regression of the observed-versus-predicted values both before and after the Bayesian step. Inspection of the PK data of liposomal amphotericin B in rabbits suggested that the volume of distribution contracted with time, as recently described by us in children (19).

$$\frac{dX_1}{dt} = R_1 - \left(\frac{CL_S}{X_3} + K_{cp} \right) \times X_1 + K_{pc} \times X_2 \quad (5)$$

$$\frac{dX_2}{dt} = K_{cp} \times X_1 - K_{pc} \times X_2 \quad (6)$$

$$\frac{dX_3}{dt} = -X_3 \times K + V_{\text{fin}} \quad (7)$$

with output equation

$$Y_1 = X_1 / X_3 \quad (8)$$

where X_1 and X_2 are the amounts of liposomal amphotericin B in the central and peripheral compartments, respectively. CL_S is the clearance of drug from the central compartment, and K_{cp} and K_{pc} are the two first-order intercompartmental rate constants connecting the central (c) and peripheral (p) compartments. X_3 is the volume of the central compartment that contracts with time according to equation 7. X_3 has an initial volume, V_{ini} , which is estimated as an initial condition in Pmetrics. The volume contracts over time according to the first-order rate constant, K . The final volume after prolonged drug administration is V_{fin} . Y_1 is ●●. Equation 5 describes the rate of change of the amount of liposomal amphotericin B in the central compartment. Equation 6 describes the rate of change of the amount of liposomal amphotericin B in the peripheral compartment.

PK-PD bridging studies. In order to place the experimental findings in a clinical context, we bridged the preclinical PK-PD findings from mice and rabbits to patients using a previously described population PK model for liposomal amphotericin B (20). This model was used to estimate the average drug exposure (quantified in terms of AUC) resulting from various human doses.

ACKNOWLEDGMENTS

We acknowledge the helpful contributions of Andrew Sharp and Joanne Goodwin.

REFERENCES

1. Jarvis JN, Bicanic T, Loyse A, Namarika D, Jackson A, Nussbaum JC, Longley N, Muzoora C, Phulusa J, Taseera K, Kanyembe C, Wilson D, Hosseinipour MC, Brouwer AE, Limmathurotsakul D, White N, van der Horst C, Wood R, Meintjes G, Bradley J, Jaffar S, Harrison T. 2014. Determinants of mortality in a combined cohort of 501 patients with HIV-associated cryptococcal meningitis: implications for improving outcomes. *Clin Infect Dis* 58:736–745. <https://doi.org/10.1093/cid/cit794>.
2. Bicanic T, Muzoora C, Brouwer AE, Meintjes G, Longley N, Taseera K, Rebe K, Loyse A, Jarvis J, Bekker LG, Wood R, Limmathurotsakul D, Chierakul W, Stepniewska K, White NJ, Jaffar S, Harrison TS. 2009. Independent association between rate of clearance of infection and clinical outcome of HIV-associated cryptococcal meningitis: analysis of a combined cohort of 262 patients. *Clin Infect Dis* 49:702–709. <https://doi.org/10.1086/604716>.
3. Al-Nakeeb Z, Petraitis V, Goodwin J, Petraitiene R, Walsh TJ, Hope WW. 2015. Pharmacodynamics of amphotericin B deoxycholate, amphotericin B lipid complex, and liposomal amphotericin B against *Aspergillus fumigatus*. *Antimicrob Agents Chemother* 59:2735–2745. <https://doi.org/10.1128/AAC.04723-14>.
4. Lestner JM, Howard SJ, Goodwin J, Gregson L, Majithiya J, Walsh TJ, Jensen GM, Hope WW. 2010. Pharmacokinetics and pharmacodynamics of amphotericin B deoxycholate, liposomal amphotericin B, and amphotericin B lipid complex in an in vitro model of invasive pulmonary aspergillosis. *Antimicrob Agents Chemother* 54:3432–3441. <https://doi.org/10.1128/AAC.01586-09>.
5. Bicanic T, Bottomley C, Loyse A, Brouwer AE, Muzoora C, Taseera K, Jackson A, Phulusa J, Hosseinipour MC, van der Horst C, Limmathurotsakul D, Meintjes G, Bradley J, Jaffar S, Harrison T. 2014. Determinants of mortality in a combined cohort of 501 patients with HIV-associated cryptococcal meningitis: implications for improving outcomes. *Clin Infect Dis* 58:736–745. <https://doi.org/10.1093/cid/cit794>.

- rotsakul D, White NJ, Wilson D, Wood R, Meintjes G, Harrison TS, Jarvis JN. 2015. Toxicity of amphotericin B deoxycholate-based induction therapy in patients with HIV-associated cryptococcal meningitis. *Antimicrob Agents Chemother* 59:7224–7231. <https://doi.org/10.1128/AAC.01698-15>.
6. Wingard JR, Kubilis P, Lee L, Yee G, White M, Walshe L, Bowden R, Anaissie E, Hiemenz J, Lister J. 1999. Clinical significance of nephrotoxicity in patients treated with amphotericin B for suspected or proven aspergillosis. *Clin Infect Dis* 29:1402–1407. <https://doi.org/10.1086/313498>.
 7. Longley N, Muzoora C, Taseera K, Mwesigye J, Rwebembera J, Chakera A, Wall E, Andia I, Jaffar S, Harrison TS. 2008. Dose response effect of high-dose fluconazole for HIV-associated cryptococcal meningitis in southwestern Uganda. *Clin Infect Dis* 47:1556–1561. <https://doi.org/10.1086/593194>.
 8. Nussbaum JC, Jackson A, Namarika D, Phulusa J, Kenala J, Kanyemba C, Jarvis JN, Jaffar S, Hosseinipour MC, Kamwendo D, van der Horst CM, Harrison TS. 2010. Combination flucytosine and high-dose fluconazole compared with fluconazole monotherapy for the treatment of cryptococcal meningitis: a randomized trial in Malawi. *Clin Infect Dis* 50:338–344. <https://doi.org/10.1086/649861>.
 9. Hamill RJ, Sobel JD, El-Sadr W, Johnson PC, Graybill JR, Javaly K, Barker DE. 2010. Comparison of 2 doses of liposomal amphotericin B and conventional amphotericin B deoxycholate for treatment of AIDS-associated acute cryptococcal meningitis: a randomized, double-blind clinical trial of efficacy and safety. *Clin Infect Dis* 51:225–232. <https://doi.org/10.1086/653606>.
 10. O'Connor L, Livermore J, Sharp AD, Goodwin J, Gregson L, Howard SJ, Felton TW, Schwartz JA, Neely MN, Harrison TS, Perfect JR, Hope WW. 2013. Pharmacodynamics of liposomal amphotericin B and flucytosine for cryptococcal meningoencephalitis: safe and effective regimens for immunocompromised patients. *J Infect Dis* 208:351–361. <https://doi.org/10.1093/infdis/jit164>.
 11. Perfect JR, Dismukes WE, Dromer F, Goldman DL, Graybill JR, Hamill RJ, Harrison TS, Larsen RA, Lortholary O, Nguyen MH, Pappas PG, Powderly WG, Singh N, Sobel JD, Sorrell TC. 2010. Clinical practice guidelines for the management of cryptococcal disease: 2010 update by the Infectious Diseases Society of America. *Clin Infect Dis* 50:291–322. <https://doi.org/10.1086/649858>.
 12. Sloan DJ, Dedicoat MJ, Laloo DG. 2009. Treatment of cryptococcal meningitis in resource limited settings. *Curr Opin Infect Dis* 22:455–463. <https://doi.org/10.1097/QCO.0b013e32832fa214>.
 13. Livermore J, Howard SJ, Sharp AD, Goodwin J, Gregson L, Felton T, Schwartz JA, Walker C, Moser B, Muller W, Harrison TS, Perfect JR, Hope WW. 2014. Efficacy of an abbreviated induction regimen of amphotericin B deoxycholate for cryptococcal meningoencephalitis: 3 days of therapy is equivalent to 14 days. *mBio* 5:e00725-13. <https://doi.org/10.1128/mBio.00725-13>.
 14. Muzoora CK, Kabanda T, Ortu G, Ssentamu J, Hearn P, Mwesigye J, Longley N, Jarvis JN, Jaffar S, Harrison TS. 2012. Short course amphotericin B with high dose fluconazole for HIV-associated cryptococcal meningitis. *J Infect* 64:76–81. <https://doi.org/10.1016/j.jinf.2011.10.014>.
 15. Perfect JR, Lang SD, Durack DT. 1980. Chronic cryptococcal meningitis: a new experimental model in rabbits. *Am J Pathol* 101:177–194.
 16. Sudan A, Livermore J, Howard SJ, Al-Nakeeb Z, Sharp A, Goodwin J, Gregson L, Warn PA, Felton TW, Perfect JR, Harrison TS, Hope WW. 2013. Pharmacokinetics and pharmacodynamics of fluconazole for cryptococcal meningoencephalitis: implications for antifungal therapy and in vitro susceptibility breakpoints. *Antimicrob Agents Chemother* 57:2793–2800. <https://doi.org/10.1128/AAC.00216-13>.
 17. Day JN, Chau TT, Laloo DG. 2013. Combination antifungal therapy for cryptococcal meningitis. *N Engl J Med* 368:2522–2523. <https://doi.org/10.1056/NEJMc1305981>.
 18. Drusano GL. 2005. Infection site concentrations: their therapeutic importance and the macrolide and macrolide-like class of antibiotics. *Pharmacotherapy* 25:150S–158S. <https://doi.org/10.1592/phco.2005.25.12part2.150S>.
 19. Lestner JM, Groll AH, Aljayyousi G, Seibel NL, Shad A, Gonzalez C, Wood LV, Jarosinski PF, Walsh TJ, Hope WW. 2016. Population pharmacokinetics of liposomal amphotericin B in immunocompromised children. *Antimicrob Agents Chemother* 60:7340–7346. <https://doi.org/10.1128/AAC.01427-16>.
 20. Hope WW, Goodwin J, Felton TW, Ellis M, Stevens DA. 2012. Population pharmacokinetics of conventional and intermittent dosing of liposomal amphotericin B in adults: a first critical step for rational design of innovative regimens. *Antimicrob Agents Chemother* 56:5303–5308. <https://doi.org/10.1128/AAC.00933-12>.
 21. Warner DF, Mizrahi V. 2014. Shortening treatment for tuberculosis—to basics. *N Engl J Med* 371:1642–1643. <https://doi.org/10.1056/NEJMe1410977>.
 22. Clemons KV, Schwartz JA, Stevens DA. 2012. Experimental central nervous system aspergillosis therapy: efficacy, drug levels and localization, immunohistopathology, and toxicity. *Antimicrob Agents Chemother* 56:4439–4449. <https://doi.org/10.1128/AAC.06015-11>.
 23. Smith PJ, Olson JA, Constable D, Schwartz J, Proffitt RT, Adler-Moore JP. 2007. Effects of dosing regimen on accumulation, retention and prophylactic efficacy of liposomal amphotericin B. *J Antimicrob Chemother* 59:941–951. <https://doi.org/10.1093/jac/dkm077>.
 24. Neely MN, van Guilder MG, Yamada WM, Schumitzky A, Jelliffe RW. 2012. Accurate detection of outliers and subpopulations with Pmetrics, a nonparametric and parametric pharmacometric modeling and simulation package for R. *Ther Drug Monit* 34:467–476. <https://doi.org/10.1097/FTD.0b013e31825c4ba6>.

AUTHOR QUERIES

AUTHOR PLEASE ANSWER ALL QUERIES

1

AQau—Please confirm the given-names and surnames are identified properly by the colors.

■ = Given-Name, ■ = Surname

AQaff—Please confirm the following full affiliations or correct here as necessary. This is what will appear in the online HTML version:

^aAntimicrobial Pharmacodynamics and Therapeutics, Department of Molecular and Clinical Pharmacology, University of Liverpool, Liverpool, United Kingdom

^bCharles River Laboratories, Davis, California, USA

^cDepartment of Medicine, Duke University, Durham, North Carolina, USA

^dResearch Centre for Infection and Immunity, St. George's University of London, London, United Kingdom

AQaff—This affiliation line will appear in the PDF version of the article and matches that on page 1 of the proof; corrections to this affiliation line may be made here or on page 1 of the proof:

Antimicrobial Pharmacodynamics and Therapeutics, Department of Molecular and Clinical Pharmacology, University of Liverpool, Liverpool, United Kingdom^a; Charles River Laboratories, Davis, California, USA^b; Department of Medicine, Duke University, Durham, North Carolina, USA^c; Research Centre for Infection and Immunity, St. George's University of London, London, United Kingdom^d

AQA—Please confirm accuracy of all added definitions, including those of PK parameters.

AQB—Please proofread entire article carefully, as not all minor edits have been queried. Also check renumbered references (necessary since Materials and Methods were moved to the end of the article per ASM style).

AQC—Please clarify sense of “milligram-milligram basis” – do you mean “milligram by milligram basis”?

AQD—Change of “Dose-exposure-response” to “Dose exposure-response” correct? i.e., relationship of the exposure to a dose and the response?

AQE—“AUC:MIC” change to “AUC/MIC ratio” correct? See similar changes throughout. If not correct, please clarify meaning of AUC:MIC.

AQF—Note that Fig. 2 and 3 have been renumbered to ensure correct numerical order in the text. Also in the next paragraph, citation of original Fig. 3 has been changed to Fig. 4 – correct?

AQG—ASM style requires that abbreviations be introduced at first occurrence of the terms, but subsequent reintroduction is permitted per ASM style.

AQH—Sentence beginning “The fungal densities ...” correct as edited?

AUTHOR QUERIES

AUTHOR PLEASE ANSWER ALL QUERIES

2

AQI—"homogenates of cerebrum" change to "homogenates of cerebral tissue" correct?

AQJ—"the mouse may" change to "the mouse studies may" correct?

AQK—Please clarify specific meaning of "4+" or delete if possible since it doesn't appear elsewhere.

AQL—Please proofread all display equations carefully for accuracy and add parentheses and brackets, if appropriate, to indicate the order of operations. Also, confirm accuracy of definitions of PK parameters for all display equations.

AQM—ASM style requires that numbered display equations be numbered sequentially throughout the article, so this second batch of equations have been renumbered; please check accuracy of citation of equations 5 to 8 throughout.

AQN—Please define Y_1 .

AQO—"The AUC/MIC ratio ..." sentence correct as edited?
